Science of Sintering, **50** (2018) 433-443

doi: https://doi.org/10.2298/SOS1804433T

UDK 546.284; 621.315.612; 53.086

Dense lanthanum silicate oxyapatite ceramics obtained by uniaxial pressing and slip casting

Ramiro Moreira Toja[1*)], Nicolás M. Rendtorffa[2], Esteban F. Agliettia[2], Tetsuo Uchikoshi[3], Yoshio Sakka[3], Gustavo Suáreza[2]

[1]Centro de Tecnología de Recursos Minerales y Cerámica (CETMIC), Camino Centenario y 506, M.B. Gonnet C.C.49 (B1897ZCA), Argentina.

[2]Departamento de Química, Facultad de Ciencias Exactas- UNLP, Calle 115 y 47, La Plata (1900), Argentina.

[3]National Institute for Materials Science (NIMS), Tsukuba, Ibaraki 305-0047, Japan.

Abstract:

Lanthanum silicate oxyapatite (LSO) is a promising ion conductive ceramic material, which has higher oxygen ion conductivity at intermediate temperatures (600–800 °C) compared to yttria-stabilized zirconia. Its mechanical properties, though important for any of its applications, have been scarcely reported. In this study, we compare apparent densification, open porosity and Vickers hardness of samples conformed by uniaxial pressing and slip casting and fired up to 1600 °C. Colloidal processing was optimized for slip casting in order to get high green densities. At sintering temperatures higher than 1400 ºC, both processing routes yielded comparable densities, although uniaxially pressed samples show slightly better mechanical properties, evidencing that slip cast ones already underwent a grain growth process.

Keywords*: Apatite-type lanthanum silicates; Uniaxial pressing; Slip casting; Sintering; Microstructure.*

1. Introduction

Alternative electrical power generation has always been the driving force for many research lines. Solid oxide fuel cells (SOFCs) have been the objective of many research fields where the search for new electrolytes has begun to target alternative structure types seeking low emission of pollutants and high energy conversion efficiency. Commercial fuel cells systems based on oxygen conduction electrolytes show yttria-stabilized zirconia (YSZ) as the oxide-conducting electrolyte due to its high oxide ion conductivity at high temperatures (800–1000 °C). Recently, the trend is to shift the operational temperatures to lower temperatures in order to avoid problems as high cost, difficult cell sealing and the low lifetime of the components caused by the high operation temperature [1, 2]. Furthermore, solid electrolytes may suffer cracking during cell operation due to their poor toughness and strength [2], making their mechanical behavior an important matter to take into account.

Lanthanum silicate oxyapatite (LSO) has recently appeared as a promising ion conductive ceramic material for its use in SOFCs. It's structure is that of apatites, with a formula of $La_{9.33+x}(SiO_4)_6O_{2+3x/2}$, where x ranges from 0 to 0.66 [3]. LSO attracted attention after Nakayama et al. reported, in 1995, high oxygen ion conductivity in rare earth silicate

*) **Corresponding author:** rmtoja@cetmic.unlp.edu.ar

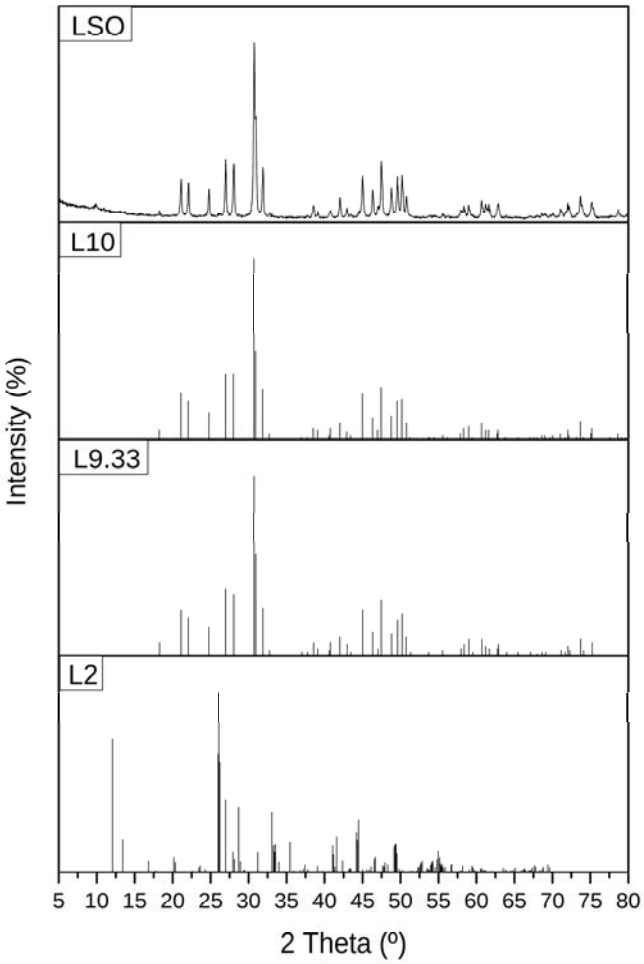

Fig. 1. XRD patterns of LSO synthesized powder, and $La_{9.33}(SiO_4)_6O_2$ (named L9.33), $La_{10}(SiO_4)_6O_3$ (named L10) and $La_2O_7Si_2$ (named L2) reference patterns.

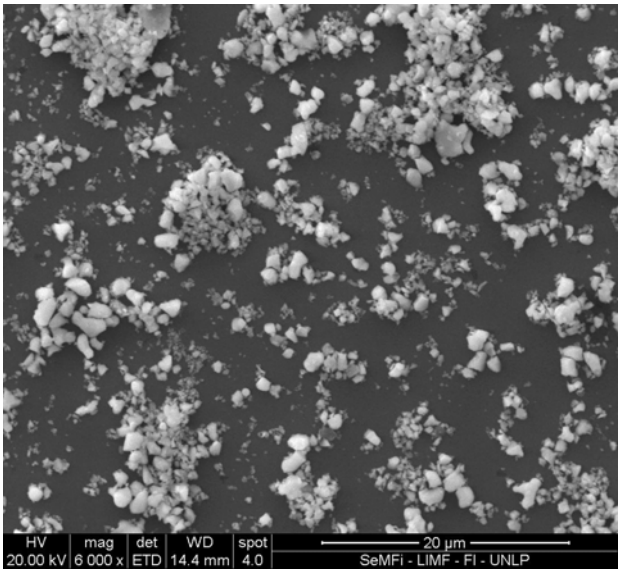

Fig. 2. SEM micrograph of LSO powder.

oxyapatites [4, 5]. Interest in LSO is due to its higher oxygen ion conductivity compared to YSZ at intermediate temperatures (600–800 °C) [6, 7], becoming a possible replacement as solid electrolyte in SOFCs. Operation of fuel cells at lower temperatures could reduce operation costs, and LSO particularly would suffer from a decreased chemical wear compared to YSZ [8] Unlike YSZ, which depends on oxide vacancies to be conductive, LSO exhibits oxide ionic conduction via interstitial conduction [6, 9, 10].

Panteix et al. [11] showed that a high densification of final samples significantly improves conductivity. In this field, there have been efforts to reduce sintering temperatures required to obtain dense materials [1, 12-16], but there is still a way to go to improve densification. Previous work has been done in our group in relation to processing and sintering dense materials by using electrophoretic deposition (EPD) [12].

Final properties of ceramic materials are signed by the processing route, where, for example, in order to obtain full dense materials it is necessary to increase the sintering temperature or time, for porosity to be eliminated and grain growth to occur[17, 18]. Different techniques have been performed in order to obtain dense LSO materials from synthesized powders, as uniaxial pressing, electrophoretic deposition or plasma spraying [12-14] Each technique comes with its own pros and cons for different applications. Despite the variety of previous studies, none of them compared two of the most common techniques for ceramics processing, slip casting and uniaxial pressing, which are also two of the most usual ones for industrial application.

Technologically speaking, it should be considered the real need for complex processing routes. Although both uniaxial pressing and slip casting is commonly used, the former is simpler and more scalable and doesn't involve the optimization of dispersion's parameters, i.e. weight content, use of dispersants, rheology, etc. If materials with similar properties can be obtained via both routes, even if it implies sintering at higher temperatures or for longer periods of time for uniaxially pressed samples, dealing with slip casting's requirements may not be worthwhile.

In this study, we compare apparent densification, open porosity and Vickers hardness of samples conformed by uniaxial pressing and slip casting from dispersions with varying dispersant concentration.

2. Experimental Procedure

2.1. Material

Reagent grade $La(OH)_3$ and SiO_2 powders were dispersed in distilled water to prepare $La_{9.33}Si_6O_{26}$ precursor. The precursor was dried at 100 °C, crushed and calcined thrice at 1400 °C for 10 h in air. The calcined powder was finally crushed to obtain a powder. The synthesis process used to obtain the ceramic powder is described elsewhere [13].

2.2. Powder characterization

The crystalline phases and crystalline structure formed were analyzed by powder XRD analysis (Philips PW 3710 equipment with Cu-Kα radiation in Ni filter at 40 kV–35 mA, with 2θ between 5 and 80 °, 2 s per steps of 0.04°).

Aqueous dispersions of LSO powder were prepared for each relative concentration of Dolapix CE-64, starting from non-addition (0 % of dispersant), 0.2, 0.3 and 0.4 wt%, and their ζ potentials at varying pH were studied with a Brookhaven Particle Size Analyzer 90Plus equipment.

The same suspensions at pH 9 were analyzed by a static light scattering equipment (Malvern Mastersizer 2000) and its average particle size distribution was measured.

Direct observation of powder's grain size and morphology was performed by scanning electron microscope (FEI Quanta200). Particle size was measured from SEM micrographs using Image J software [19].

2.3. Forming

2.3.1. Uniaxial pressing

Disk shape samples of 1.5 g each were grinded with a mortar and uniaxially pressed at 100 MPa, in order to avoid a preferential orientation leading to lamination and lower final densities. This samples will be named UP.

2.3.2. Slip casting

Water dispersions of the powder with 60 %wt solid loading were prepared at pH 9 with varying dispersant (Dolapix CE-64) concentration: 0.2, 0.3 and 0.4 wt% respect to solids, named 0.2D, 0.3D, 0.4D respectively, in a similar fashion as Badiee et al [20]. Disk-shaped samples were slip cast from these dispersions. Suspensions with no dispersant addition were not possible to be prepared.

2.4. Sintering

Both uniaxially pressed and slip casted samples were sintered at temperatures of 1300, 1400, 1500, 1550 and 1600 °C in an electric furnace with heating rates of 5 °C/min and a dwell time of 2 hours, in an air atmosphere.

2.5. Sample characterization

Density and porosity of both green and sintered pieces were determined by the Archimedes method, using kerosene and water, respectively. Vickers hardness (Hv) was evaluated by the indentation method on a polished surface with Buehler IndentaMet 1100 equipment at 0.3 Kg for 15 s [21].

Final polished samples were thermally etched and their microstructures were observed by scanning electron microscope (FEI Quanta200). Grain size was measured from SEM micrographs using ImageJ software [19].

3. Results and Discussion

Fig. 1 shows the XRD pattern of the LSO synthesized powder, as well as reported patterns for $La_{9.33}(SiO_4)_6O_2$ (PDF 00-049-0443), $La_{10}(SiO_4)_6O_3$ (PDF 00-053-0291) and $La_2O_7Si_2$ (PDF 01-082-0729). It can be seen that it's hard to differentiate between $La_{9.33}(SiO_4)_6O_2$ and $La_{10}(SiO_4)_6O_3$, as they share a great amount of features. The presence of small features between 26.0° and 26.3° imply the presence of a minimum percentage of $La_2O_7Si_2$ phase. The synthesized powder is in agreement with the desired phase $La_{9.33+2x}(SiO_4)_6O_{2+3x}$ ($0<x<0.33$).

Fig. 2 shows a SEM micrograph of the as synthesized powder. It can be seen that particles don't present a regular shape nor size, but they share general characteristics such as straight edges.

Fig. 3 shows the particle size distribution. It can be seen that the majority of particles (~ 60 %) have a size between 0.2 and 0.6 μm. The mean diameter is 0.51 μm ± 0.33 μm evidencing the wide distribution of particles.

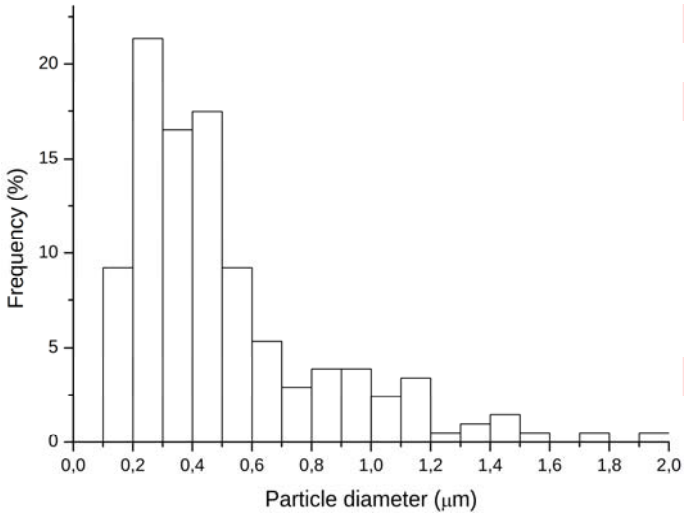

Fig. 3. Particle size distribution.

Fig. 4 shows the ζ potential curves of all different suspensions prepared. It can be seen that ζ potential is negative at the whole range of pH, and in particular in a range of pH from 9 to 11, it is large enough (≈ -30 mV) to assure the dispersion stability.

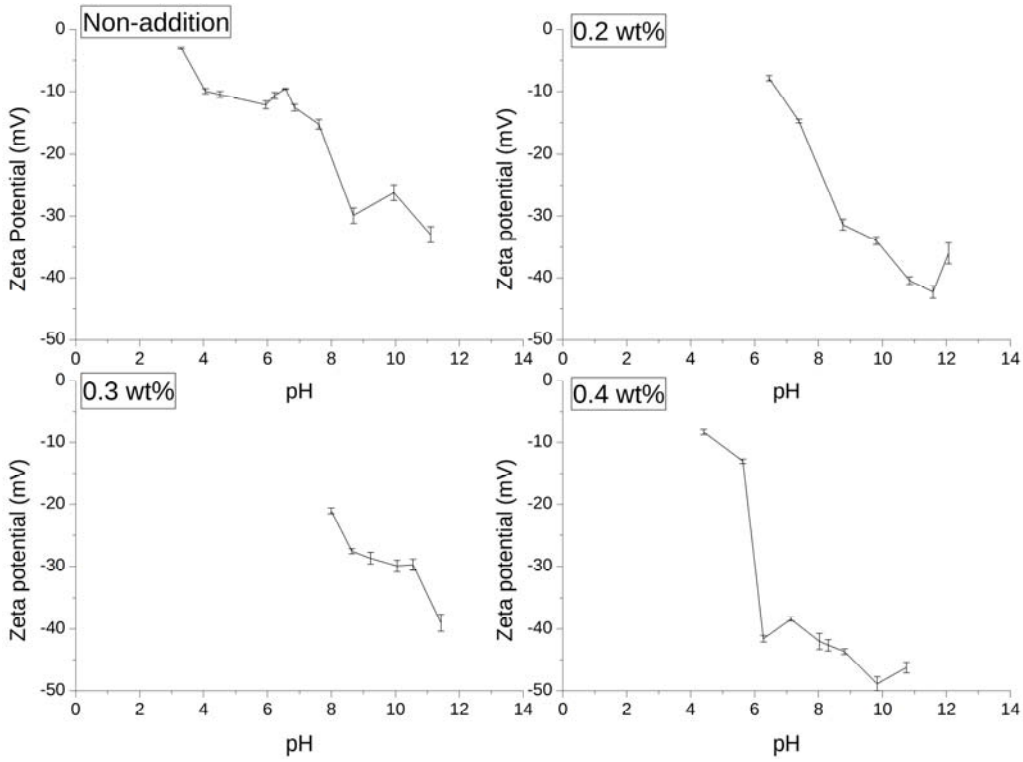

Fig. 4. ζ potential vs pH of aqueous dispersions of LSO containing no dispersant added, and dispersant contents of 0.2 wt%, 0.3 wt% and 0.4 wt%.

Particle size distribution was also studied for an LSO powder dispersion and dispersions containing different amounts of Dolapix CE-64 dispersant. It is generally described by maximum particle size for given percentages of sample; i.e. lower decil, median and upper decil (d(0.1), d(0.5) and d(0.9), respectively). These three parameters are reported for the aforementioned dispersions in Tab. I. It can be seen that the addition of dispersant greatly diminishes the agglomeration of particles. There's a minor but noticeable difference in d(90) between 0.2D and both 0.3D and 0.4D.

Tab. I Particle size distribution for aqueous dispersions (pH=9) of LSO containing no dispersant added, and dispersant contents of 0.2, 0.3 and 0.4 wt%.

Content of dispersant	**d(0,1) (µm)**	**d(0,5) (µm)**	**d(0,9) (µm)**
0.0%	0.58	2.22	68.63
0.2%	0.12	0.21	1.34
0.3%	0.11	0.21	1.48
0.4%	0.11	0.21	1.47

The dispersant, which makes the particle surface negatively charged, will keep the particles non-agglomerated in the suspension in the mentioned range of pH. The amount of dispersant is important for two reasons, one is to avoid the existence of an uncovered particle surface and the other is to avoid excess of it, which can generate bridging effect of the polyelectrolyte causing agglomeration as well as larger porosity while the dispersant is calcined during the sintering process. It can be observed from Tab. I that, in the studied range, the amount of dispersant does not significantly affect the average particle size. The ζ potential is directly related to the observed particle size: when ζ potential's absolute value is large, particles experience a higher repulsion and agglomeration is less favorable, thus the observed particle size is smaller.

In spite of observing no variation in d(50) for the studied range of dispersant content, it is preferable to minimize the dispersant content, as bigger contents of organic compounds will cause a detriment in final density. For this reason, the suspensions optimal dispersant content is 0.2 wt%.

Fig. 5 shows the apparent density and the open porosity of both uniaxially pressed and slip casted green samples, calculated via Archimedes method in kerosene. Due to not being able to determine the prescence of only one phase from XRD patterns, green density is shown as an absolute value, and not a percent density relative to theoretical density. It can be seen that colloidal processing is a proper technique to prepare materials which final goal is to sinter up to full densification, if adequately dispersant content is found. However, for large amount of dispersant (0.4 wt%), green density is lower than those obtained by uniaxial pressing.

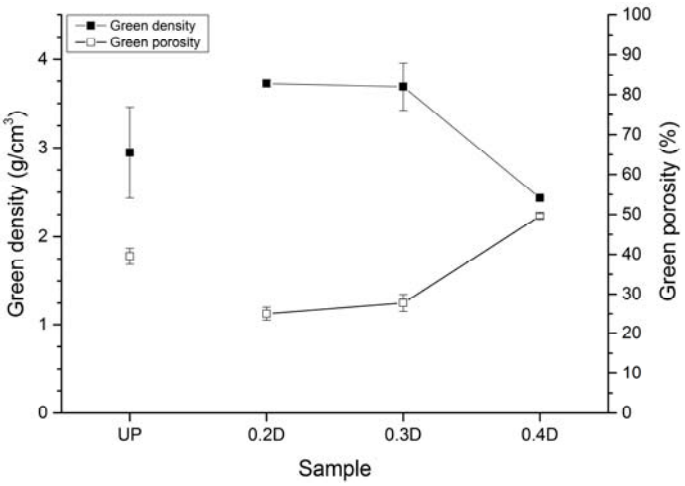

Fig. 5. Apparent density and open porosity of green samples for UP, 0.2D, 0.3D and 0.4D. Closed marks show green density and open marks show green porosity.

Fig. 6 shows the sintering behavior of all samples. As discussed for green density, final sintered density is not shown as relative density but as absolute density instead.. It can be seen that density and apparent porosity come to a dwell after 1500 °C. UP samples reach a density larger than 5.1 g/cm^3 at 1550 °C, while 0.2D and 0.3D samples overcome the 5.1 g/cm^3 density threshold at 1500 °C. Meanwhile, 0.4D samples can only reach this density at 1600 °C.

It can be seen that slip casted samples sinter at lower temperatures than the uniaxial pressed ones. At 1500 °C the density of slip casted samples already reached the maximum densification while the uniaxially pressed ones are still under densification.

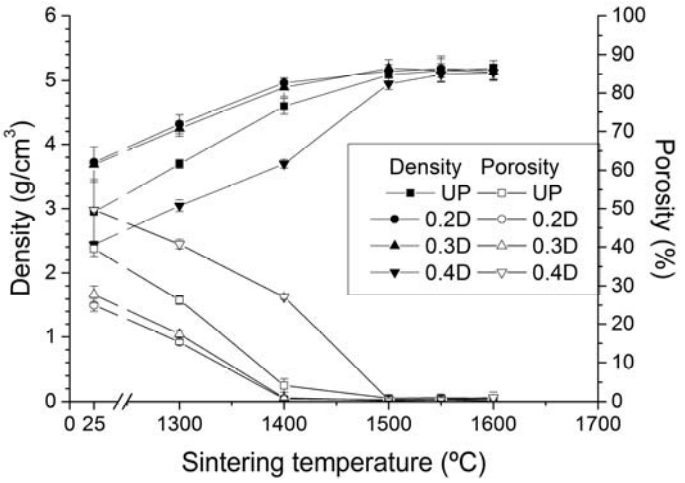

Fig. 6. Textural properties of green and dense LSO casted samples. Closed marks show density and open marks show porosity.

Fig. 7 shows the microstructure for 0.2D and UP samples sintered at 1300, 1500 and 1600 °C. These samples were chosen to favor a comparison between uniaxial pressing and slip casting, taking into account representative temperatures for the sintering behavior. It can be seen that the UP sample sintered at 1300 °C presents the highest porosity of all considered samples. UP sample sintered at 1500 °C shows the biggest grain size. Both UP and 0.2D samples sintered at 1500 and 1600 °C show a lack of uniformity in grain size.

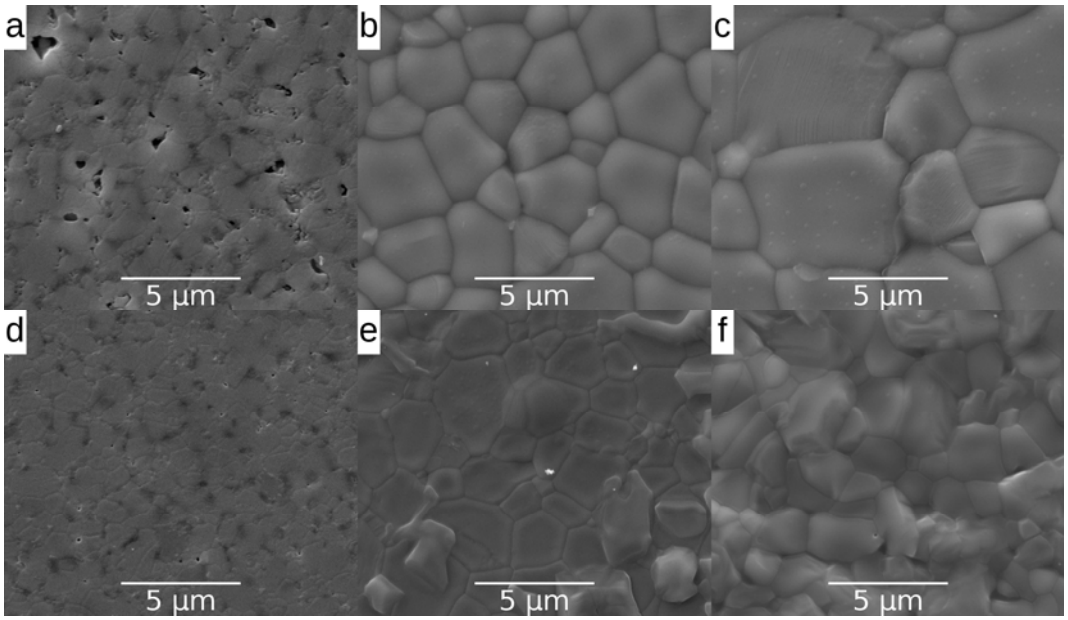

Fig. 7. SEM micrographs of: a, b and c, UP samples sintered at 1300, 1500 and 1600 °C, respectively, and d, e and f, 0.2D samples sintered at 1300, 1500 and 1600 °C, respectively.

Fig. 8 and Fig. 9 show the mean grain size and grain size distribution, respectively, for 0.2D and UP samples sintered at 1300, 1500 and 1600 °C, measured from SEM images. It could be said that grain size reaches a maximum for 0.2D samples sintered at 1500 °C, and then decrease for samples sintered at 1600 °C; nevertheless, they are in the same order. UP sample sintered at 1600 °C shows the biggest grain size. It can be seen that as sintering temperature grows, grain size distribution becomes more disperse and reaches larger sizes. It can also be noted that 0.2D samples are less disperse than UP samples, which means that grain size is more homogeneous. This is generally viewed as advantageous for obtaining good mechanical performance.

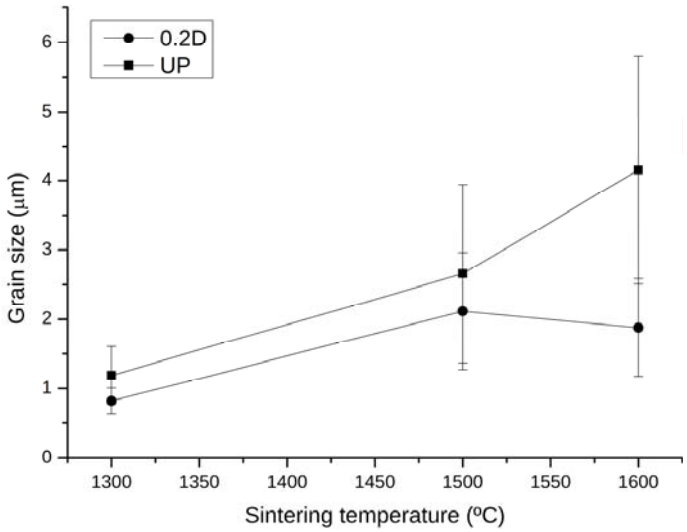

Fig. 8. Mean grain size of UP and 0.2D samples sintered at 1300, 1500 and 1600 °C.

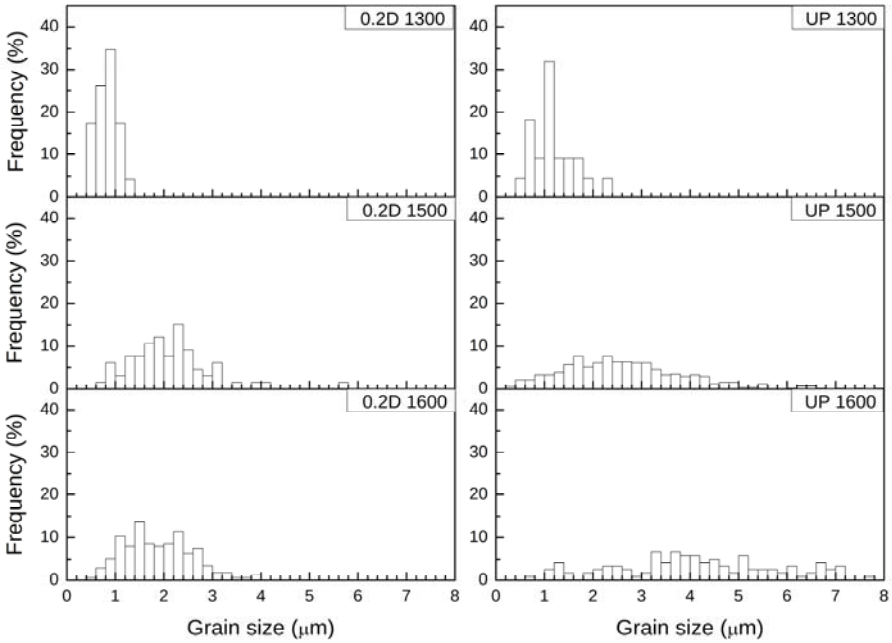

Fig. 9. Grain size distribution of UP and 0.2D samples sintered at 1300, 1500 and 1600 °C.

Fig. 10 shows the Vickers hardness for UP and 0.2D samples sintered at different temperatures. It can be seen that hardness for both UP and 0.2D samples show the same general behavior: it grows with sintering temperature, reaches a maximum and finally diminishes. This is in agreement with grain size and apparent density measurements: Vickers hardness grows during densification but finally diminishes due to grain growth. 0.2D samples reaching their highest Vickers hardness at a lower sintering temperature than UP samples indicates that 0.2D reaches higher densification at lesser temperatures, in accordance to our previous discussion.

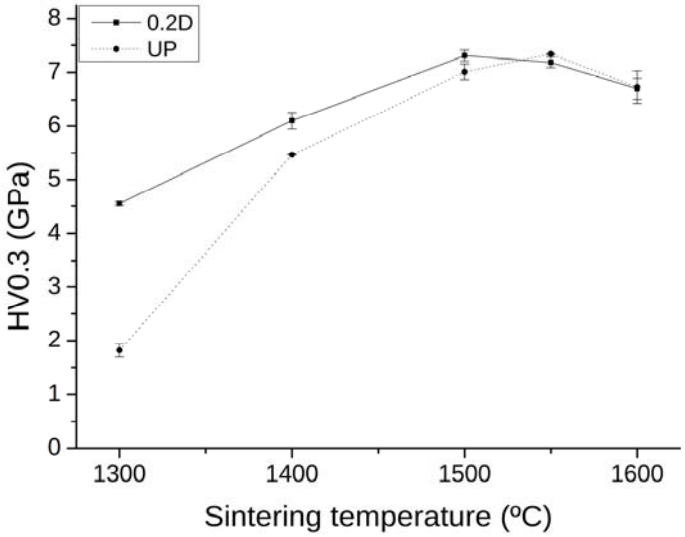

Fig. 10. Vickers hardness of UP and 0.2D samples sintered at 1300, 1400, 1500, 1550 and 1600 °C.

4. Conclusion

In this study we investigated two common ceramic processing routes for obtaining lanthanum silicate oxyapatite pieces. The results show that both routes can be used to obtain dense ceramics, with a porosity near 0 %. In addition, colloidal processing was optimized for slip casting, being a 0.2 %wt content of Dolapix CE-64 the optimal dispersant content in order to get high green densities.

Slip casted samples reached significantly higher densities and lower porosities up to a sintering temperature of 1400 °C than uniaxially pressed samples. At higher sintering temperatures, both processing routes yielded comparable densities, although uniaxially pressed samples show slightly better mechanical properties, evidencing that slip casted samples already underwent a grain growth process.

Both processing routes show technical advantages and disadvantages: uniaxial pressing is easier to scale-up, but needs higher temperatures to fully sinterize, meanwhile slip casted samples reach final density at lower temperatures but previous colloidal processing needs a better control than uniaxial pressing conditions.

Acknowledgments

The authors would like to thank CONICET for the scholarship granted to RMT and to ANPCyT for the fundings (PICT 2013-1102). RMT would also like to thank Lic. S. Conconi for the fruitful discussion related to XRD analysis.

5. References

1. J. M. Porras-Vázquez, E. R. Losilla, L. León-Reina, D. Marrero-López, M. A. G. Aranda, J. Am. Ceram. Soc. 92 (5) (2009) 1062.
2. Y. H. Liu, C. Q. Yin, L. H. Wang, D. B. Li, J. S. Lian, J. D. Hu, Z. X. Guo, Sci. Sinter. 40 (1) (2008) 13.
3. W. Gao, G. Yin, H. Yin, H. Zhu, X. Wu, L. Zhong, M. Sun, R. Cong, J. Zhang, Q. Cui, J. Alloys Compd. 586 (2014) 279.
4. S. Nakayama, T. Kageyama, H. Aono, Y. Sadaoka, J. Mater. Chem. 5 (11) (1995) 1801.
5. S. Nakayama, H. Aono, Y. Sadaoka, Chem. Lett. 24 (6) (1995) 431.
6. P. R. Slater, J. E. H. Sansom, J. R. Tolchard, Chem. Rec. 4 (6) (2004) 373.
7. K. Kobayashi, Y. Sakka, J. Ceram. Soc. Jpn. 122 (1431) (2014) 921.
8. A. M. Misso, D. R. Elias, F. dos Santos, C. Yamagata, Adv. Mater. Res. 975 (2014) 143.
9. K. Kobayashi, Y. Matsushita, M. Tanaka, Y. Katsuya, C. Nishimura, Y. Sakka, Solid State Ion. 225 (2012) 443.
10. K. Kobayashi, T. S. Suzuki, T. Uchikoshi, Y. Sakka, Solid State Ion. 258 (2014) 24.
11. P. J. Panteix, I. Julien, P. Abélard, D. Bernache-Assollant, Ceram. Int. 34 (7) (2008) 1579.
12. G. Suarez, N. T. K. Nguyen, N. M. Rendtorff, Y. Sakka, T. Uchikoshi, Ceram. Int. 42 (16) (2016) 19283.
13. K. Kobayashi, K. Hirai, T. S. Suzuki, T. Uchikoshi, T. Akashi, Y. Sakka, J. Ceram. Soc. Jpn. 123 (1436) (2015) 274.

14. W. Gao, H. Liao, C. Coddet, Appl. Surf. Sci. 254 (17) (2008) 5548.
15. S. Celerier, C. Laberty-Robert, F. Ansart, C. Calmet, P. Stevens, J. Eur. Ceram. Soc. 25 (12) (2005) 2665.
16. Y. Ma, M. Moliere, Z. Yu, N. Fenineche, O. Elkedim, J. Alloys Compd. 723 (2017) 418.
17. M. R. Gauna, M. S. Conconi, G. Suarez, E. F. Aglietti, N. M. Rendtorff, Sci. Sinter. 49 (2018) 15.
18. M. Mazaheri, Z. R. Hesabi, F. Golestani-Fard, S. Mollazadeh, S. Jafari, S. K. Sadrnezhaad, J. Am. Ceram. Soc. 92 (5) (2009) 990.
19. C. A. Schneider, W. S. Rasband, K. W. Eliceiri, Nat. Methods 9 (7),2012, 671.
20. S. H. Badiee, S. Otroj, M. Rahmani, Sci. Sinter. 44 (3) (2012) 341.
21. S. Gómez, G. Suárez, N. Rendtorff, E. Aglietti, Sci. Sinter. 48 (1) (2016) 119.

Садржај: *Лантан силикат оксоапатит (LSO) је јонски проводљиви керамички материјал, који има већу проводљивост на средњим температурама (600–800 °C) у поређењу са цирконијумом. У раду су приказана механичка својства. Упоређивали смо густину, отворену порозност и тврдоћу по Викерсу узорака добијених униаксијалним пресовањем и изливањем а затим синтеровањем до 1600 °C. На температурама синтеровања изнад 1400 ºC, обе методе су дале одговарајуће густине. Узорци добијени пресовањем су позали боља механичка својства указујући на то да је узорак изливањем већ прошао фазу раста зрна.*

Кључне речи: *силикати, униаксијално пресовање, ливење, синтеровање, микроструктура.*